



Characterisation of pyrolysis and combustion parameters of charring materials most frequently found in buildings

Ariza S. Abu-Bakar¹ · Marlene J. Cran³ · Rahul Wadhvani^{2,3} · Khalid A. M. Moinuddin^{2,3} 

Received: 12 February 2019 / Accepted: 9 August 2019 / Published online: 26 August 2019
© Akadémiai Kiadó, Budapest, Hungary 2019

Abstract

A comprehensive study has been conducted on some charring materials frequently found in buildings to characterise pyrolysis and combustion parameters concerning the variations in heating rate, temperature and heat flux. Since these parameters are input for computational fluid dynamics (CFD)-based fire models, incorporation of the effects of heating rate and heat flux when simulating building fires may lead to better predictions of tenability conditions. Three common construction and building materials were selected, namely pine, cotton and wool, to characterise via experimental protocols which can serve as examples of future novel charring materials. Parameter values related to pyrolysis reactions were determined using thermogravimetric analysis and differential scanning calorimetry. The values of the combustion parameters were obtained using cone calorimetry. It was found that the variation in heating rate has a significant effect on the values of the pyrolysis parameters of the studied materials. The kinetic parameter and heat of reaction (HoR) values of pine increased with the increment in heating rate. Conversely, the kinetic parameter values of cotton and wool decreased as the heating rate increased, whereas the HoR values followed a similar incremental trend with the increasing heating rate. The variation in combustion parameter values varied concerning heat flux due to the presence of high moisture contents and possible variations in char development in all materials. As CFD-based fire models are currently widely used to design and assess performance-based building fire safety designs, to obtain better predictions of tenability conditions, a proposal for the optimised use of parameters is presented.

Keywords Pyrolysis · Combustion · Chemical kinetics · Heating rate · Temperature · Heat flux

Introduction

The performance-based building fire safety design method is preferred by fire engineers and researchers due to the flexibility offered to the user to adopt their new design concept without compromising safety aspects required by regulation. As experimental studies are vastly expensive, numerical simulation is an alternative method to test building fire safety designs. Computational fluid dynamics (CFD)-based fire models are widely used to simulate a number of probable fire scenarios to assess how long buildings remain tenable for occupants and firefighters. As outlined in a previous study [1], a set of “fire properties” is required for each combustible material frequently found in buildings to simulate pyrolysis where material decomposition occurs as a result of the release of gases and other volatiles, and combustion which is an exothermic gas-phase reaction between gaseous fuel and oxygen [2]. A compartment fire grows from the time of ignition which

Electronic supplementary material The online version of this article (<https://doi.org/10.1007/s10973-019-08688-6>) contains supplementary material, which is available to authorized users.

✉ Khalid A. M. Moinuddin
khalid.moinuddin@vu.edu.au

¹ School of Housing, Building and Planning, Universiti Sains Malaysia, 11800 USM, Penang, Malaysia

² Centre for Environmental Safety and Risk Engineering, Victoria University, PO Box 14428, Melbourne, VIC 8001, Australia

³ Institute for Sustainable Industries and Liveable Cities, Victoria University, PO Box 14428, Melbourne, VIC 8001, Australia

results in temperature rise and its rate of rising in materials present, both combustible and non-combustible, as well as the rise in the incident radiation upon the materials. It has been observed that the values of a number of fire properties vary concerning temperature, heating rate and incident radiation, although some are nominally constant [3]. All of these fire properties are required as input parameters for CFD-based fire models such as fire dynamic simulator (FDS) [4]. Examples of modelling, with fire properties (obtained at single heating rate and single incident radiation), of burning construction materials with FDS can be found in [5, 6].

This study is motivated to enable a fire engineer/researcher to obtain and quantify the representative pyrolysis and combustion parameters with respect to temperature, heating rate, and incident radiation of unknown or novel charring materials. Once these parameters are characterised, these can be provided as fire properties as input variables in a CFD-based fire model for coupled pyrolysis and combustion simulation. An example without variations can be seen in [7]. Such characterisation and application will assist in the better prediction of the fire scenarios and deteriorating tenability conditions on which performance-based fire safety design can be assessed. The secondary aim of this study is to propose a method for the optimised use of those parameters. In a previous study [1], the characterisation of fire properties of a non-charring material (polymethyl methacrylate, PMMA) for CFD-based fire model was presented. PMMA is a synthetic polymer that is widely used in building construction particularly for windows, doors, skylight roofing, and bath enclosures. Following on, the objective of this study is to similarly characterise some important fire properties of charring materials frequently found in buildings as an example of future novel charring materials.

In this study, pine, cotton and wool were considered. Pine is widely used in building constructions due to its versatility in structural and decorative applications. It is widely used in flooring, ceilings, doors, window frames and furniture, with applications ranging from the basics such as plywood and panelling to more complicated such as joinery, cladding, decking, fencing and furniture. Fabric-based furnishing materials are not only the source of fuel but also the contributor to the spread of flames in the room [3]. The composition of fabric materials is highly variable with natural materials such as cotton or wool fabrics or their blends commonly used in curtains and furnishing. These materials enhance the interiors of buildings due to the wide variety of colours and designs. However, fabrics are generally fast to ignite in fires and quickly respond to heat exposure. Thus, a detailed study of the flammability and kinetic parameters of these charring materials is beneficial to understand the fire behaviour under various

conditions. There is a scarcity of such literature which provides the variation in data with the major factors affecting it. This study may lead to better predictions of outcomes in building fires with such important data for current materials and provide a methodology for characterising unknown or novel charring materials.

Materials and methods

Material preparation

The materials used in this study included cotton, wool and radiata pine. Hundred per cent of wool and cotton content with approximate densities of 211 and 254 kg m⁻³, respectively, and Australian radiata pine with a density of 442 ± 30 kg m⁻³ were used in this study. Pine was sourced from a local prominent hardware store, and fabrics were sourced from a local prominent furnishing store. All materials were untreated. The parameters related to pyrolysis reactions also known kinetic parameters (activation energy, *E*, pre-exponential factor, *A*, reaction order, *n*, char yield and heat of reaction, HoR) were determined using thermogravimetric analysis (TGA) and differential scanning calorimetry (DSC). A Perkin Elmer TGA7 (PTGA) and a Mettler Toledo TGA/DSC1 STARe system (MTGA) were used for the TGA study, and a Mettler Toledo DSC1 STARe system (MDSC) was used for the DSC study. For DSC and TGA measurements, the pine, cotton and wool samples were cut into small pieces measuring approximately 1 × 1 × 1 mm for pine and 1 × 1 × 0.5 mm for fabrics. Test summary is presented in Table 1.

The combustion parameters were obtained using: (1) ultimate analysis to determine chemical composition and stoichiometry of the combustible materials and (2) cone calorimetry to obtain the yield of primary combustion products (i.e. CO, CO₂, soot and char) and the effective heat of combustion (EHOc). It is to be noted that micro-scale combustion calorimetry (MCC) can also be used to characterise combustion parameters [8]; however, characterisation using cone calorimetry is more conventional for large-scale flame spread modelling.

Chemical compositions of studied materials are presented in Table 2. Carbon–hydrogens content in these materials, in principle, determines the combustion heat. It can be observed that wool contains significant amount of sulphur which has inhibitory effects on the combustion process.

A cone calorimeter manufactured by Fire Testing Technology, UK, was used in this study for obtaining combustion parameters, and for these experiments, slabs of pine measuring 100 × 100 × 25 mm were prepared,

Table 1 Summary of pyrolysis and combustion parameters measured

Parameters	Pyrolysis parameters			Combustion parameters						
	A	E	n	Char residue (non-flaming)	HoR	EHoC	Soot yield	CO yield	Soot yield	Char residue (flaming)
Equipment	TGA				TGA/DSC	Cone calorimeter				
Sample size (mm)	~ 1 mm × 1 mm (pine) ~ 0.5 mm × 0.5 mm (Cotton, Wool)					Pine: 100 mm × 100 mm × 25 mm Cotton, wool: 100 mm × 100 mm × 0.5 mm				
Heating rate (K min ⁻¹)	Pine: 5, 10, 20, 30, 50, 100, 200 Cotton: 5, 10, 50, 100, 200 Wool: 5, 10, 20, 30, 40, 50, 100, 200					NA				
Irradiance (kW m ⁻²)	NA					Pine: 20, 30, 40, 50, 75 Cotton: 30, 40, 50, 75 Wool: 30, 40, 50, 75				

Table 2 Chemical compositions of studied materials

Element/%	Pine ^a	Cotton ^b	Wool ^c
Carbon	54.9	40.7	50.5
Hydrogen	5.8	5.6	6.8
Oxygen	39.0	45.2	22.0
Nitrogen	0.2		16.5
Others	0.1 (S)	~8.5 (N, ash, H ₂ O)	3.7 (S) 0.5 (ash)
Carbon-to-oxygen ratio	1.4	0.9	2.3

^aRagland et al. [9], ^bMoriana et al. [10], ^cBauer et al. [11]

and for fabrics, the sample was set up as shown in Figure 10 in the supplementary material. An aluminium foil frame was prepared to hold the fabric, and a wire grid was placed on top of the sample following the guidelines [12]. Since fabrics are very low in mass, this provides better attachment to the backing pad as outlined by Tata, Alongi [13] and same sample thickness (single layer) was also used in the study. Tata, Alongi [13] also studied the effect of sample thickness of polyester fabric by layering 0.5 mm thick sample—with one, five and ten layers and received different time-to-ignition and peak of HRRPUA values. We used single layer as it is the likely way a fabric can be found in a building such as curtain and furnishing of furniture. Jiang [3] also used single-layer fabrics for cone calorimeter study. The samples used in all of the aforementioned measurements were conditioned for 48 h with 50% relative humidity at 23 °C. At least three runs were carried out for each test to obtain consistent results.

Measurement methods

The TGA and DSC tests were conducted under non-isothermal conditions, and the nitrogen flow was set at 50 mL min⁻¹ to induce pyrolysis. This represents a pyrolysis process where the material is tested in the absence of air. This usually occurs when there is a flaming combustion reaction preventing air reaching the burning material. Samples of 5 mg were prepared for the PTGA and DSC experiments, and heating rates between 5 and 200 K min⁻¹ were employed for all experiments. However, the MTGA required a larger sample size of ~ 20 mg which is likely to give the correct kinetic parameters. Abubakar and Moinuddin [14] showed that the sample mass is unlikely to influence kinetic parameters and similar masses have also been used in other studies [15, 16]. However, the MTGA experiments were only used for deriving some kinetic parameters. Matched data from the PTGA and MDSC were used for calculating HoR, and test data from the MTGA were also used to identify any differences in thermal lag between the PTGA and MDSC. The pine, cotton and wool samples were tested from 20 to 75 kW m⁻² irradiance levels [17] using the cone calorimeter.

Theory and calculation

A detailed theory of flammability and kinetic parameters was presented in a previous study [1]. When a sample is heated, it undergoes various physical and chemical changes. The physical changes may include melting or solid-phase transitions [18], and the chemical changes include molecular bond breakage which results in either endothermic or exothermic reactions. Examples of these

changes occur during sample pyrolysis which converts organic materials into both a solid phase (char) and gas phase [19] which is the case for materials such as pine.

Pyrolysis parameter values represent the solid-phase reaction that results in and during the burning of a material with these kinetic parameters, E , n , and A , also known as the kinetic triplet. The value of E is the minimum amount of energy required to start a chemical reaction, A is the frequency of the collisions between molecules and n is the index or exponent, to which its concentration term in the chemical reaction rate equation is raised.

As reported in [1], in this study the kinetic triplets were derived from the differential thermogravimetric (DTG) plots as shown in Fig. 1a using the inflection point method [20]. The inflection point method is used as it assists in showing the effect of heating rate on the values of kinetic triplets. Furthermore, this method has a robust ability to analyse the whole set of TGA data to determine the kinetic triplet of the sample. This method is based on the employment of a linear plot and the coefficients of the linear equation. It is well known that there is a strong interdependence among the kinetic triplet [21, 22]. Thus, for either pyrolysis modelling within CFD-based fire models like FDS or analytical calculation, the set of kinetic triplets is sufficient to reproduce TGA data instead of true values of each parameter. Figure 4 of [1] shows that different sets of kinetic triplets obtained from two different studies using two different methods could analytically generate almost identical thermogravimetric (TG) profiles for PMMA (non-charring) by applying to the Arrhenius equation. The Arrhenius equation is given by:

$$k = Ae^{\frac{-E}{RT}} \quad (1)$$

where k is the reaction rate constant (1 s^{-1}), A is the pre-exponential factor (1 s^{-1}), E is the activation energy (kJ mol^{-1}), R is the universal gas constant ($8.314 \times 10^{-3} \text{ kJ mol}^{-1} \text{ K}^{-1}$) and T is the temperature (K).

Similarly, Figure 7.1 of [23] shows that for pine (charring) almost identical DTG profiles were obtained when

different sets of kinetic triplets obtained from two different studies using two different methods ([21] and inflection method) were used. Matala [24] used an optimisation technique [21] to study the kinetics of the experimental raw data. In this technique, an optimisation algorithm performs combinatorics to estimate the values of A , E and n . Then, with each set of kinetic values, simulations are run using a pyrolysis model with values of the model that match the best with the experimental result which are taken as the “model-specific” values. These are not true values as they may or may not be universally applied to all models, and therefore, a different set of kinetic triplet values were obtained [24]. This method also provides a separate set of kinetic triplets for each heating rate. Both examples (PMMA and pine) confirm the interdependence of kinetic triplets. Therefore, to parameterise CFD-based fire models, the inflection point method used in this study is appropriate.

A protocol for HoR was presented in [1] where both the initial sample masses and the heating rates are the same for both TGA and DSC measurements. Both DSC and TGA data are matched at the same temperature, and respective heat flow measured by the DSC data is then divided by the un-subtracted mass from the TGA. These data (heat flow/mass vs. temperature) are plotted, and the HoR is determined by calculating area under the curve, where pyrolysis occurred, according to Eq. (2):

$$\Delta H_R = \frac{\Delta H_{DSC} \cdot W \cdot y_i}{x_i W} = \frac{\Delta H_{DSC} \cdot y_i}{x_i} \quad (2)$$

where ΔH_R is the HoR, ΔH_{DSC} is the normalised enthalpy, W is the total mass of the sample, y_i is the instantaneous yield of gaseous products (fraction of solid fuel) and x_i is the instantaneous fractional mass loss. To obtain ΔH_{DSC} , the definite integral should be evaluated between the temperature range on which the reaction occurs:

$$\Delta H_{DSC} = \int_{T_1}^{T_2} \frac{\Delta E}{W_i} dT \quad (3)$$

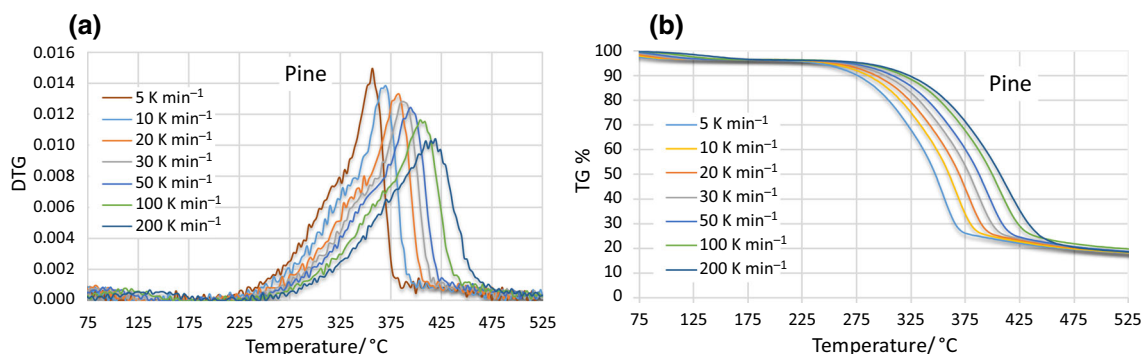
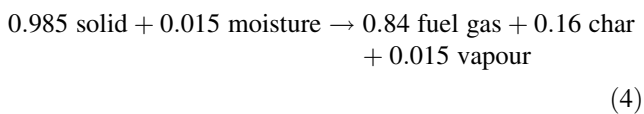


Fig. 1 Thermal data for pine using the MTGA at various heating rates: **a** DTG plot and **b** TGA curves

where ΔE is the instantaneous heat flow into the sample and w_i is the instantaneous mass.

In Eq. (2), values of y_i and x_i for non-charring materials are equal to unity. However, for charring materials, two reactions normally occur where the first is attributed to the moisture release and the second reaction is a product of fuel gas and char. Thus, the reaction path needs to be estimated as shown in the example presented in Eq. (4), where $y_i = 0.84$ and $x_i = 0.985 \times 0.84 = 0.827$.



MATLAB scripts were written to obtain the pyrolysis parameters. On the other hand, cone calorimeter's in-built software was used to obtain the flammability parameters. From regular measurements in each cone calorimeter test, combustion parameter values were averaged over 6 min from the ignition at each irradiation level for pine. For cotton and wool, the combustion period ranged from approximately 16 to 46 s and 22 to 89 s, respectively, depending on heat flux, and this may be due to a thin layer of the fabrics that are low in mass. Char yield was determined using the initial mass, final mass and moisture content with Eq. (5):

$$\text{char yield} = \frac{W_{fc}}{W_{ic}(1 - MC)} \quad (5)$$

where W_{fc} and W_{ic} are the final mass and initial mass of the sample in the cone calorimeter experiment, respectively, and MC is the moisture content obtained from the TGA experiment.

Results and discussion

Characterisation of pyrolysis parameters

Kinetic triplets of pine

For pine, the kinetic triplets were derived from Fig. 1a using the inflection point method [20] and these are presented in Fig. 2a–c as a function of heating rates (dT/dt). These figures show that the values of A , E and n vary with dT/dt which is consistent with the decomposition shift observed in Fig. 1a.

By conducting the least square regression analyses, correlations were developed and are presented in Table 3 which show that increasing linear trends are observed for the kinetic triplets with the heating rate.

Alternative pyrolysis parameters of pine

The FDS model [4] offers an alternative method for calculating the conversion rate by using a combination of the DTG peak location (REFERENCE_TEMPERATURE), peak value (REFERENCE_RATE = peak $dY/dT \times$ heating rate) and PYROLYSIS_RANGE (approximate width of the curves in Fig. 1a assuming its shape to be roughly triangular).

The values of these parameters from the DTG curves are presented as a function of the heating rate for pine and moisture in Fig. 2d–f, and the regression analyses of all three parameters for both pine and pine (moisture) show power trends. The pine pyrolysis range has shown good agreement with other studies [25–30], particularly at 10 K min^{-1} where the value of $161 \text{ }^\circ\text{C}$ is consistent with that of Wadhvani et al. [29] who reported $160 \text{ }^\circ\text{C}$. At 5 K min^{-1} , the pyrolysis range of the present study was $154 \text{ }^\circ\text{C}$, whereas Slopicka [28] obtained a value of $150 \text{ }^\circ\text{C}$ and at 2 K min^{-1} , the pyrolysis range of this study was $147 \text{ }^\circ\text{C}$ compared to $140 \text{ }^\circ\text{C}$ reported by Yao et al. [30].

Other kinetic parameters, i.e. the yield of solid residue (v_s range) and the initial mass fraction, appear to be constant concerning the heating rate for pine from the TG plots of Fig. 1b. The values of these parameters are summarised in Table 4.

HoR of pine

The HoR is an effective model parameter to account for heat loss during a pyrolysis process for the range of materials tested. The HoR values as a function of the heating rate for pine are presented in Fig. 3, and it can be observed that a very strong increasing power relationship exists for pine. An increasing trend of HoR values with respect to heating rate has also been reported for the heating of waste materials [31]. Anca-Couce et al. [32] reported a HoR value for pine of around 200 kJ kg^{-1} measured at 10 K min^{-1} , and this is higher than the value of 137 kJ kg^{-1} obtained in the current study measured at 20 K min^{-1} .

In a comprehensive review of the literature, Haseli et al. [33] concluded that the external heating rate of the material is one of the primary reasons for HoR variations. At high heating rates, more energy is required to volatilise the solid material into the gaseous phase, whereas at lower heating rates, the transition from solid to gas is via a liquid phase which requires lower energy [34].

The additional heat flow needed for volatilisation at high heating rate is further discussed by other researchers who have proposed explanations for the observed decomposition shift. Based on their study of cellulose, Missoum et al.

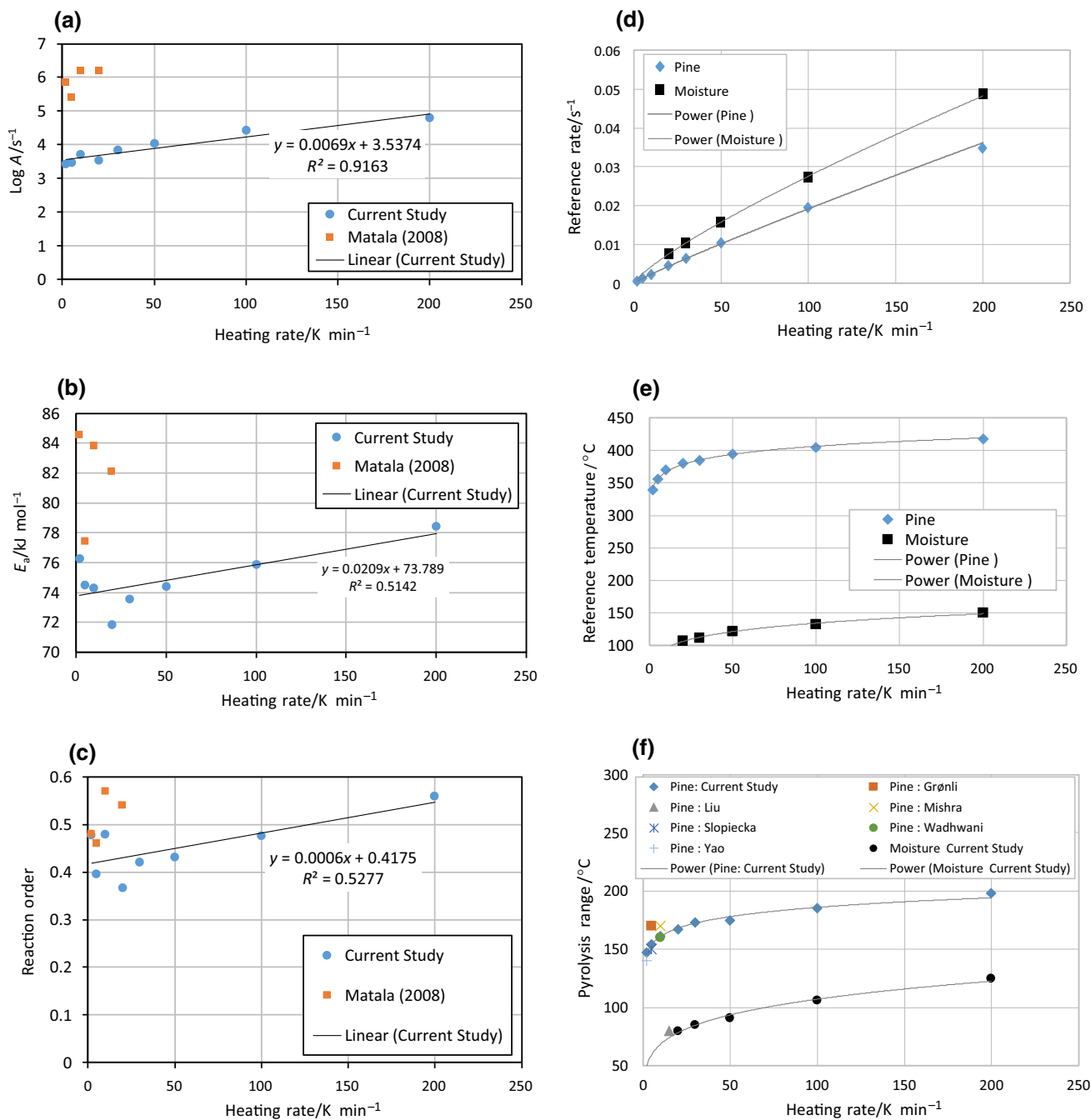


Fig. 2 Kinetic parameters: **a** natural log of pre-exponential factor (pine); **b** activation energy, E (pine); **c** reaction order, n (pine); **d** reference rate (pine and moisture); **e** Reference temperature (pine and moisture); and **f** pyrolysis range (pine and moisture)

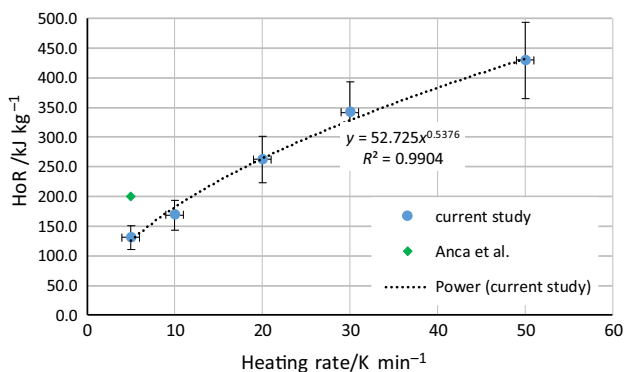
Table 3 Pyrolysis parameter correlations for pine and moisture

Parameter	Correlation for pine	Correlation for moisture
Log(A)	$0.0069 (dT/dt) + 3.5374; r^2 = 0.92$	
E	$0.021 (dT/dt) + 73.79; r^2 = 0.51$	
n	$0.0006 (dT/dt) + 0.4175; r^2 = 0.53$	
Reference rate	$0.0003 (dT/dt)^{0.9171}; r^2 = 1$	$0.0007 (dT/dt)^{0.8074}; r^2 = 1$
Reference temperature	$331.23 (dT/dt)^{0.0445}; r^2 = 1$	$68.353 (dT/dt)^{0.1467}; r^2 = 1$
Pyrolysis range	$139.41 (dT/dt)^{0.0626}; r^2 = 0.99$	$43.865 (dT/dt)^{0.194}; r^2 = 0.99$

Table 4 Yield of solid residue and initial mass fraction of pine

Material	Property	Value
Pine	Yield of solid residue	0.185
	Initial mass fraction	0.965*

*Depending on moisture content


Fig. 3 Heat of reaction (kJ kg⁻¹) for pine

[31] suggested that one reason for such a decomposition shift is the result of the decreased residence time of volatiles within the material which results in the reaction commencing at higher temperature [35]. At high heating rates, volatiles are more quickly formed and therefore they spend less time within the sample, and this can also be applicable to non-charring materials. Milosavljevic et al. [36] suggested that a “mass transport limitation”, i.e. the restriction of physical transport of the reactants at the gas–solid interface, may also be responsible for the shift in cellulosic materials.

It may be suggested that the samples have less residence time within the vicinity of any specific temperature at the higher heating rates. Therefore, by the time the volatiles are formed, the sample has reached a higher temperature, and thus, more heat flow is needed to assist the formation of volatiles quickly at higher heating rates.

Kinetic triplets and HoR of cotton and wool

According to Farooq et al. [37], the thermal decomposition of cotton can be observed over three separate stages where the first stage is the moisture release due to evaporation/dehydration. The second stage is the primary decomposition of cotton which accounts for 75% of the overall mass loss and the subsequent char formation. The third and final stage is attributed to the char removal or volatilisation of the sample. Similarly, Wakelyn et al. [38] described three stages, namely evaporation/dehydration, transformation (accounting for 2% of dry mass of sample with the

production of CO₂, CO and water vapour volatiles) and vacuum pyrolysis of pure cotton cellulose (80% of original sample mass).

The TG and DTG data for cotton are shown in Fig. 4a, b, respectively. These figures show that dehydration of cotton occurs at temperatures below 150 °C which is then followed by the pyrolysis process which takes place between 300 and 550 °C. It is clear from these figures that multiple reactions result from the pyrolysis of cotton during the measurement. Beyond this range, where the pyrolysis is completed, a char residue remains as the final product.

Overall, at each heating rate, there are three reactions: one related to moisture evaporation (termed P1) with the remaining peaks related to the pyrolysis of cotton components with the first and second peaks expressed as Cotton 1 (P2) and Cotton 2 (P3), respectively. Unfortunately, due to the reduced sensitivity of the Mettler TGA under the test conditions, the moisture peak could not be properly resolved in Fig. 4b. From Fig. 4a, it can be determined that ~ 1.2% mass loss occurred during moisture evaporation (P1), with ~ 51.2% and ~ 32.5% mass loss during P2 and P3, respectively. In this case, P2 and P3 account for ~ 84% mass loss which is roughly 10% greater than the value reported by [37]. Cao et al. [39] and references therein described 59% mass loss for cellulosic and semi-cellulosic components and 14.5% lignin (non-cellulosic) decomposition. Therefore, P2 and P3 most likely represent cellulosic and non-cellulosic decomposition, respectively. The char residue is ~ 15% and is consistent at all heating rates.

The TGA and DSC experiments enable the identification of at least two pyrolysis reactions about cotton samples P2 and P3 (cellulose and non-cellulose, respectively). However, often “single effective” kinetics is used in pyrolysis modelling due to the relative simplicity of this model. The kinetic triplet parameters derived from Fig. 4b using the inflection point method are presented in Fig. 5 for “single effective” cotton and in Figure 11 in the supplementary material for cellulose and non-cellulose kinetics as a function of heating rates (dT/dt). Through regression analysis of the reaction kinetic parameters, the empirical formulae obtained are presented in Table 5. A strong decreasing trend is observed for A and E , whereas an increasing trend is seen for n .

In Fig. 6a, the heat flow/unit mass vs temperature profile of cotton derived from the DSC and TGA data is presented by matching temperatures in the two sets of data. Here, the first peak represents moisture evaporation, the second peak represents the transformation process which absorbs heat, the third peak represents cellulose pyrolysis and the fourth peak represents non-cellulose pyrolysis. To take into account the heat absorption during transformation, the

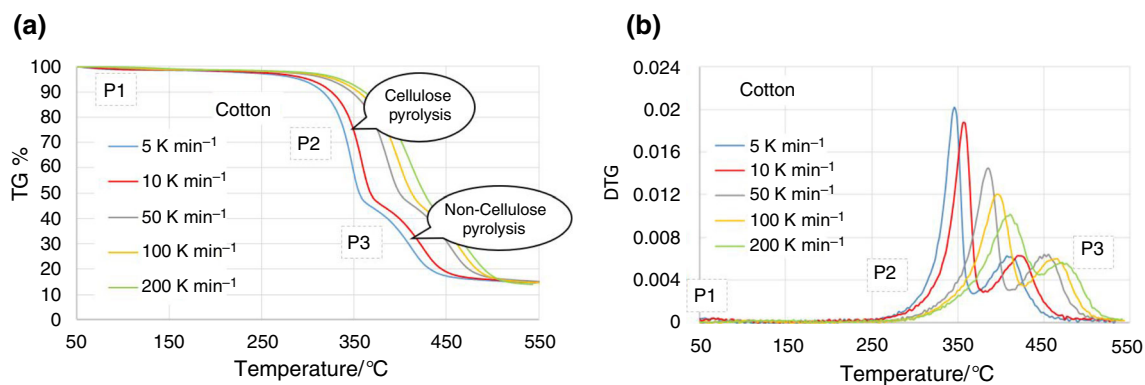


Fig. 4 Cotton **a** TGA curves; **b** DTG plot of TGA with Mettler TGA at various heating rates

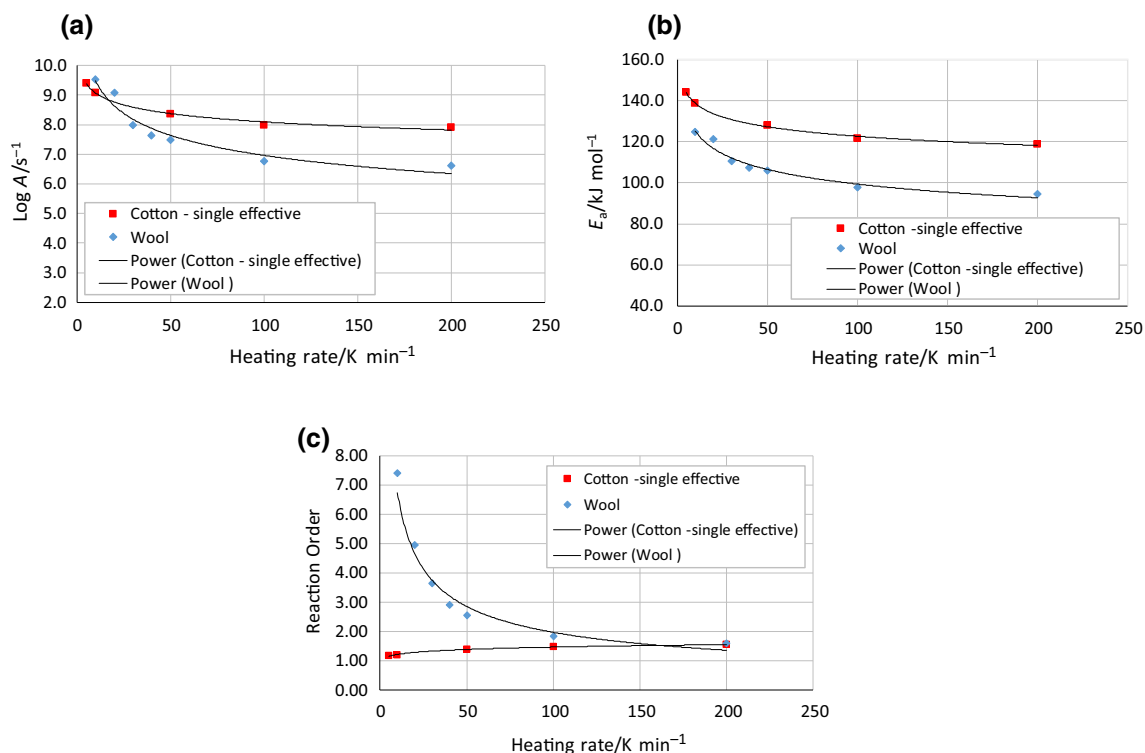


Fig. 5 Kinetic parameters of cotton and wool: **a** natural log of pre-exponential factor; **b** activation energy, E ; and **c** reaction order, n

Table 5 Pyrolysis parameter correlations (single effective) for cotton and wool

Parameter	Correlation for cotton	Correlation for wool
Log(A)	$10.164 (dT/dt)^{-0.049}$; $r^2 = 0.99$	$12.893 (dT/dt)^{-0.134}$; $r^2 = 0.94$
E	$156.75 (dT/dt)^{-0.053}$; $r^2 = 1$	$157.6 (dT/dt)^{-0.1}$; $r^2 = 0.96$
n	$1.0157 (dT/dt)^{0.081}$; $r^2 = 1$	$22.944(dT/dt)^{-0.532}$; $r^2 = 0.96$

ΔH_{DSC} for cotton cellulose obtained from the areas under the curves of the second and third peaks was separately calculated using Eq. (10) in [1] and then added in order to simplify numerical modelling. Similarly, ΔH_{DSC} for the “single effective” model includes the sum of the areas under the curves of the second, third and fourth peaks.

Conversely, the ΔH_{DSC} for non-cellulose is based only on the area under the curve of the fourth peak.

To define the area under the peaks/curves, a spline function is used whereby tangents are drawn inward from the adjacent troughs; then, they are connected with an approximate curve. Although this method is somewhat arbitrary, this conjecture is not uncommon for defining

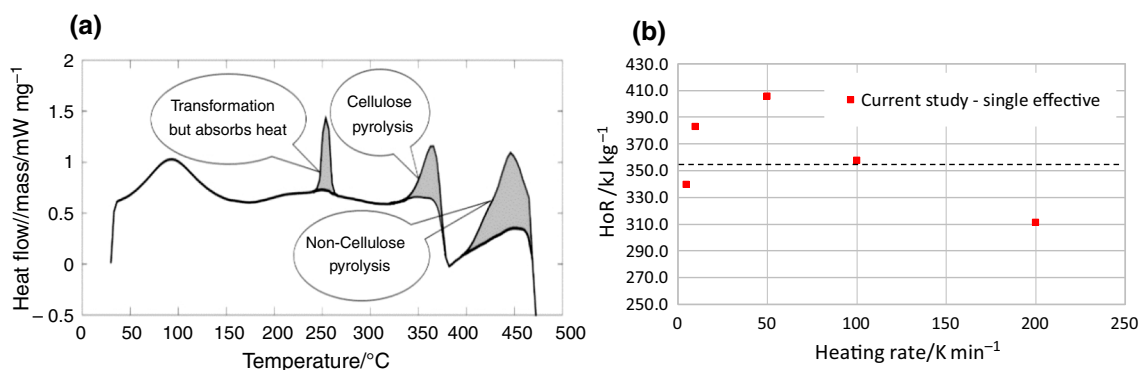


Fig. 6 **a** DSC/TGA temperature-matched heat flow/mass of cotton at 20 K min⁻¹; **b** HoR for Cotton ('single effective')

transitions in the thermal analysis [40]. The HoR values as a function of the heating rate for cotton cellulose and non-cellulose are presented in Figure 12 in the supplementary material, whereas the "single effective" model is presented in Fig. 6b. An increasing trend of HoR values concerning the heating rate for cellulose is observed, whereas a decreasing trend is seen in non-cellulose. However, no definite trend is observed for the "single effective" model.

Similar to cotton, the thermal decomposition of wool occurs in three stages [41] where the first stage is the moisture release which is due to evaporation/dehydration. The second stage is the decomposition of wool, and the final stage is attributed to the char volatilisation of the sample. Figure 7 shows the TG and DTG profiles of wool when heated from 10 to 200 K min⁻¹ over the temperature range of 50–550 °C. At lower heating rates (10–50 K min⁻¹), dehydration occurred at below 150 °C, whereas at higher heating rates, dehydration is observed just below 200 °C.

The result observed at the lower heating rate has been reported previously with the first significant TG mass loss attributed to moisture release between 30 and 120 °C [42]. This is then followed by the wool pyrolysis process over the range of approximately 200–500 °C. Horrocks and

Davies [43] reported that the pyrolysis of wool starts at 225 °C which is very close to the value found in the current study.

The results also show that a single pyrolysis reaction occurs for the wool sample and at lower heating rates (10–50 K min⁻¹) with another peak observed after pyrolysis which is attributed to the char volatilisation. Conversely, at higher heating rates, no char volatilisation is observed over the test heating range; rather, a char residue is observed as the final product of the decomposition. It is also evident that greater char residue remains at the 100 K min⁻¹ heating rate compared to the 200 K min⁻¹ heating rate (Fig. 7a). The kinetic triplet derived for a single reaction from the data of Fig. 7 using the inflection point method is presented previously in Fig. 5 as a function of heating rates (dT/dt).

The HoR for wool as a function of heating rate presented in Fig. 8b shows an increasing trend with respect to heating rate with a reasonable linear fit with some deviation from linearity at lower heating rates resulting from the regression analysis. In general, the kinetic parameters and HoR for wool show decreasing and increasing trends with increasing heating rates, respectively.

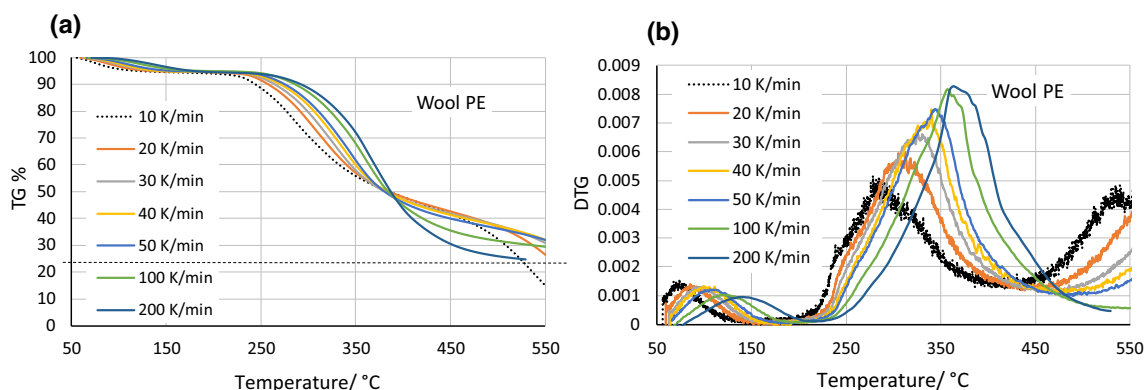


Fig. 7 Wool **a** TG (dotted line indicates char/solid residue); **b** DTG of wool obtained using Perkin Elmer TGA

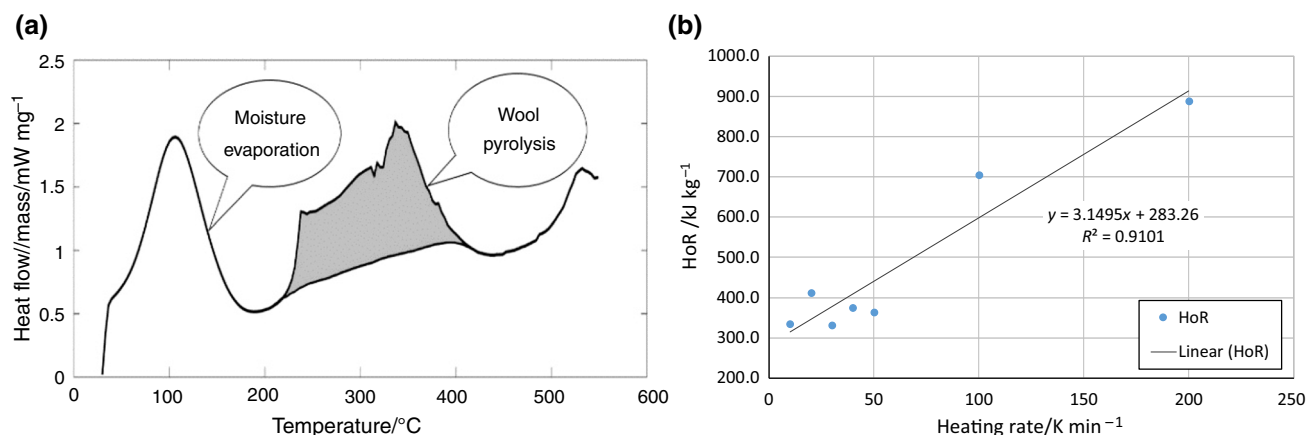


Fig. 8 Wool **a** DSC/TGA temperature-matched heat flow/mass (20 K min⁻¹) **b** HoR

For cotton, and excluding char volatilisation, the yield of solid residue (n_s) and initial mass fraction ($Y(0)$) appear to be constant with respect to heating rate (see TG plot in Fig. 4a). For wool, it appears that $Y(0)$ is independent of heating rate; however, values of n_s cannot be clearly extracted, especially at low heating rates [23]. A generalised average value of n_s was determined, and these values are given in Table 6.

It is known that changes in heating rates could have a significant effect on the pyrolysis process [38, 39]. From the DTG conversion rate profiles presented in Figs. 4b and 7b, it is evident that as the heating rates increase, the curve is also shifted to a higher temperature. A similar trend is also observed in the heat flow profile, where the heat flow also increases as the heating rate is increased. The DSC profiles also show that the peak curve shifts to higher temperatures as the heating rate increases. Furthermore, regarding the peak values, it is observed that the peak value generally increases as the heating rate is increased, indicating an increase in HoR with the increase in heating rate.

Table 6 Yield of solid residue and initial mass fraction of cotton and wool

Material	Properties	Value
Cotton	Yield of solid residue	0.143
	Initial mass fraction	0.985*
Wool	Yield of solid residue	0.275
	Initial mass fraction	0.945*

*Depending on moisture content

Characterisation of combustion parameters

Primary parameters

Significant variations in combustion parameter values as the heat flux changes are observed for all three charring materials tested. These are presented in Fig. 9 along with char residue as a function of heat flux. These values are the averaged values obtained from multiple measurements at each heat flux level. Char yield result for 20 kW m⁻² is not presented as at this irradiation sample did not completely burn; i.e. some virgin component remained unburnt. Through regression analysis of these variables, a number of empirical formulae were obtained for pine, cotton and wool and are presented in Table 7.

Linear correlations were obtained for all these parameters with strong correlations observed for the EHoC, char residue and CO₂ yield. The average EHoC measured at 50 kW m⁻² and obtained in this study, 11.21 MJ kg⁻¹, is close to study conducted by Park [44] where a value of 12.94 MJ kg⁻¹ was obtained. The CO₂ yield in the same study was 1.39 kg kg⁻¹ which is compared reasonably well to that of the current study of 1.14 kg kg⁻¹. Although there is an increasing trend for char residue with respect to heat flux with a reasonable linear fit, there is some deviation from linearity at lower heat flux. In addition, a CO yield of 0.019 kg kg⁻¹ was reported by Park [44] with a comparative value in the current study of 0.007 kg kg⁻¹. It should be noted that there are numerous pine species across the world and comparisons should be made with this consideration.

For cotton and wool samples, tests with heat fluxes lower than 30 kW m⁻² commonly resulted in different outputs when tests were repeated under the same conditions. Therefore, fabric samples were tested at a minimum

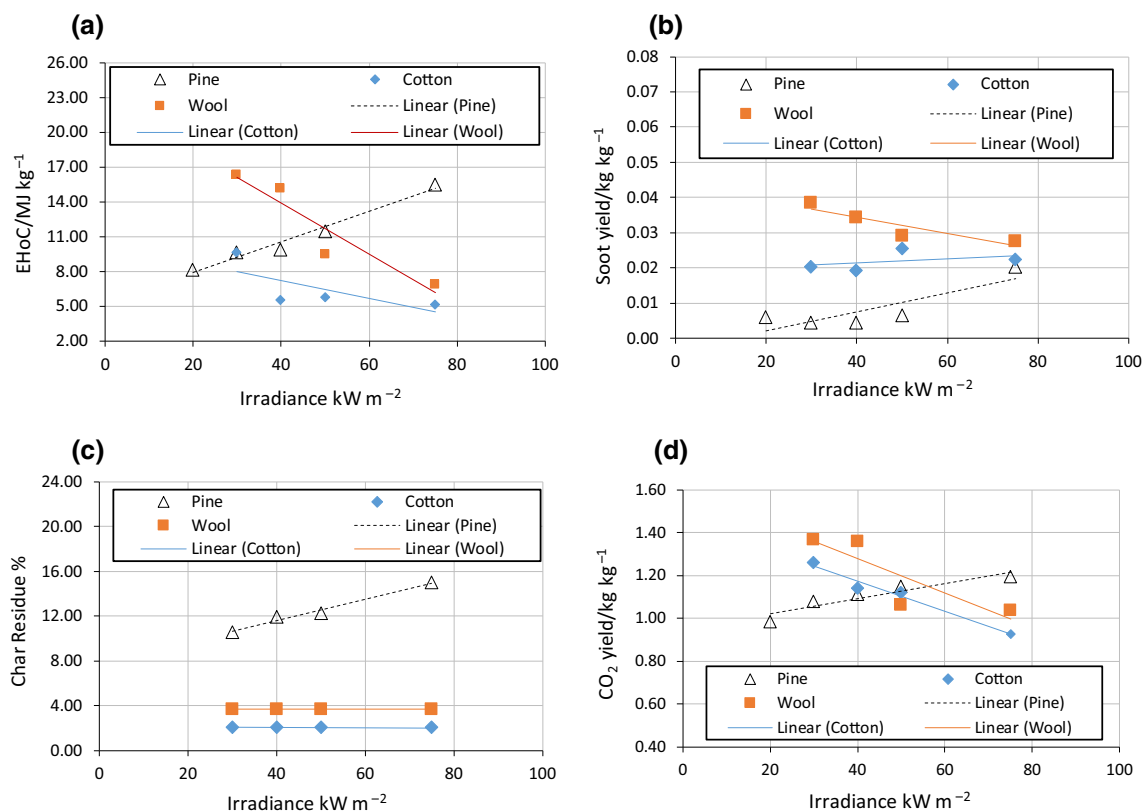


Fig. 9 a Effective heat of combustion; b Soot yield; c Char residue; d CO₂ yield with respect to heat flux

Table 7 Combustion parameter correlations for tested materials

Material	Pine	Cotton	Wool
EoHC	$0.1318 \dot{q}'' + 5.24; r^2 = 0.97$	$10.798 \dot{q}'' - 0.0011; r^2 = 0.5537$	$- 0.2214 \dot{q}'' + 22.749; r^2 = 0.886$
Soot yield	$0.0003 \dot{q}'' - 0.0034; r^2 = 0.73$	$- 6E-06 \dot{q}''^2 + 0.0007 \dot{q}'' + 0.0042; r^2 = 0.449$	$- 0.0002 \dot{q}'' + 0.0438; r^2 = 0.8139$
CO ₂ yield	$0.0035 \dot{q}'' + 0.9527; r^2 = 0.88$	$- 0.007 \dot{q}'' + 1.4548; r^2 = 0.9708$	$- 0.0081 \dot{q}'' + 1.6006; r^2 = 0.7335$
Char residue	$0.0951 \dot{q}'' + 7.81; r^2 = 0.98$	$\mu = 2.10; \sigma = 0.02$	$\mu = 3.74; \sigma = 0.02$

of 30 kW m⁻² in this study which showed good repeatability. The time- and sample-averaged values of four combustion parameters (EHoC, soot yield, char residue and CO₂ yield) obtained at 30, 40, 50 and 75 kW m⁻² irradiation from the cone calorimeter software for cotton are presented in Fig. 9. A linear correlation was obtained with a relatively good fit for the CO₂ yield, whereas a weak exponential trend was observed for EHoC as a function of heat flux with no tangible trend for the CO and soot yield data which present average values of 0.013 ± 0.0022 kg kg⁻¹ and 0.022 ± 0.003 kg kg⁻¹, respectively.

The time- and sample-averaged values of the same four (for pine and cotton) combustion parameters obtained from the cone calorimeter software as functions of heat fluxes for wool are also presented in Fig. 9. Good-to-average linear correlations were obtained for each parameter except for char residue, and in addition, the CO yield was 0.010 ± 0.0018 kg kg⁻¹. Wool shows similar behaviour to cotton under burning with the production of a char [45]. The values of char residue with respect to heat flux are presented in Fig. 9c, and no significant trend is observed.

Other combustion parameters

For simplistic fire modelling, where pyrolysis is not modelled, the heat release rate per unit area (HRRPUA) or mass loss rate per unit area (MLRPUA) can be used where these two parameters are interchangeable, i.e. $\text{MLRPUA} \times \text{EHC}$ gives the HRRPUA. Values of peak HRRPUA, averaged HRRPUA and standard deviation of HRRPUA along with correlations (as functions of radiative heat flux, q_r in kW) are presented in Table 8. At first, three sets of time-series test data were averaged. Then, averaged and standard deviation values were calculated for the averaged set from ignition to 360 s for pine and from ignition to flameout for fabrics. For cotton and wool, logarithmic relationships are obtained, whereas pine shows a linear relationship. The ignition time (T_{ign}) data are also presented in Table 8, and based on all tested materials, it can be seen that the ignition time decreased as the heat flux increased with a q_r^{-2} relationship obtained for all three materials.

Overall, for three charring materials, significant variations in parameter values with respect to the incident irradiance were observed. It is likely that the presence of high moisture contents and possible variations in char development with respect to incident radiation flux may influence these variations, especially for EHC. Additionally, moisture evaporation and char development may not be uniform through the depth of the sample during the fire test. It was also found that many parameters vary with time during the tests, even under constant irradiation.

Optimised use of parameters

As a fire grows in a real fire event, the combustible materials exposed to fire receive different irradiance levels and are heated at different rates (dT/dt). Ideally, simulations should be performed by using appropriate values for temperature, heating rate and irradiance at each computational node or cell for the fire conditions. For pyrolysis simulations, Donskoi and McElwain [46] proposed a method for altering the values of the A and E relevant to changing heating rates. In another method, Li et al. [47] coupled Kissinger's method [48] with an optimisation method to obtain a single kinetic triplet across three heating rates. The triplet was then extrapolated to a fourth heating rate, and reasonable agreement with experimental data was found. Furthermore, it is possible to determine kinetic triplets for various reaction paths or for various components within the sample by an optimisation process [49]. However, none of these methods are expanded to include the effects of HoR as a function of heating rate and are applied to fire scenarios where solid- and gas-phase reactions are coupled.

Optimisation methods are also proposed by Lautenberger et al. [21] to obtain an optimised single set of all properties including kinetic triplets and HoR to match cone calorimeter measurements, where the solid phase is directly modelled, and a fixed gas-phase heat source is considered. It would be tremendously computationally "expensive" to include the gas-phase reaction modelling in the optimisation process.

From the current study of experimental and numerical results, it appears that the method described by Donskoi and McElwain [46] can be expanded for modelling coupled solid- and gas-phase reactions by altering the values of the kinetic triplet and the HoR relevant to changing heating rates. This method for the FDS fire model by using built-in RAMP functions is described below. This RAMP function method is not limited to the kinetic triplet and HoR only, but it is also applicable to combustion parameters that can vary with incident radiation.

Ramp functions

Currently, with the RAMP function, the thermal properties (specific heat, C_p and thermal conductivity, k) can be specified as functions of temperature. The RAMP function allows users to control the behaviour of these two parameters that are found experimentally. The behaviour can be linear or nonlinear, and some examples are given below:

```

Cp_steel(T)
{
  Case 1: T= 20., F=0.45 / implies Cp=0.45 kJ kg-1 K-1 when 20°C≥T
  Case 2: T=677., F=0.85 / implies Cp=0.00083T+0.6 when 20°C≤T≤677°C and
  Cp=0.85 when T≥677°C
}

k_steel(T)
{
  Case 1: T= 20., F=48. / implies k=48 W m-1 K-1 when 20°C≥T
  Case 2: T=677., F=30. / implies k=-0.0274T+48 when 20°C≤T≤677°C and
  k=30 when T≥677°C
}

```

It should be noted that for values of temperature (1) below and above the given range, FDS will assume a constant value equal to the first or last F specified; and (2) between two consecutive temperatures, parameter values increase or decrease linearly. With this setting, the fire growth and development are being simulated by using a set of thermo-physical property values at various temperatures.

Proposed ramp functions

It was shown previously that parameter values of A , E , n and HoR vary with dT/dt for pine, cotton and wool. Similar to the approach of Donskoi and McElwain [46], provisions can be made for specifying the dT/dt -dependent values of

Table 8 HRRPUA and ignition time

Heat Flux	Cotton				Wool				Pine			
	HRRPUA/kW m ⁻²				HRRPUA/kW m ⁻²				HRRPUA/kW m ⁻²			
	Average	Peak	SD	T _{ign} /s	Average	Peak	SD	T _{ign} /s	Average	Peak	SD	T _{ign} /s
20												
30	21.75	70.41	21.84	22.0	21.56	48.72	16.49	51	68.68	125.33	24.89	164
40	34.84	73.8	26.17	9.0	35.57	96.42	34.11	23	79.63	132.11	23.03	100
50	37.48	72.37	25.56	7.5	44.79	101.48	36.49	15	84.14	142.25	24.22	35
75	37.79	76.0	26.79	3.5	55.62	109.4	37.87	7	106	188.05	31.55	19
Correlation	16.3ln(<i>q_r</i>) - 29	6ln(<i>q_r</i>) + 50		19000 <i>q_r</i> ⁻²	37ln(<i>q_r</i>) - 142	60ln(<i>q_r</i>) - 102		42000 <i>q_r</i> ⁻²	1.13 <i>q_r</i> + 45	1.85 <i>q_r</i> + 82		70000 <i>q_r</i> ⁻²
r ²	0.68	0.78		0.95	0.98	0.73		0.97	0.97	0.93		0.95

parameters in FDS. However, similar to the temperature RAMP function described above, the heating rate RAMP functions: (ACTIVATION_ENERGY_RAMP, HEAT_OF_REACTION_RAMP, PREEXPONENTIAL_FACTOR_RAMP and REACTION_ORDER_RAMP) can be used in FDS. As the heating rate increases or decreases, the RAMP function will provide appropriate material property values representing actual conditions. As the FDS calculates the temperature history of each solid cell, it is possible to calculate *dT/dt* for every time step. For simplicity, FDS may need to use parameter values of the previous time step for the current time step.

The cone calorimeter experimental results presented in Sect. 4.2 show the variation in parameter values for EHoC, CO yield, CO₂ yield and smoke yield concerning a change in radiative heat flux (especially for charring materials). As the FDS calculates radiative heat flux on each solid surface, it is possible to introduce an IRRADIANCE_RAMP function for every time step. It has been observed that those parameters vary with time during the tests even under constant irradiation. It may be argued that a more complicated algorithm needs to be developed to reflect the changes in values with respect to irradiance, time, material thickness, char fraction etc. However, the method proposed in this study can offer the first steps towards improved usage of bench-scale data. It is expected that in future, more advanced algorithms will be developed in relation to gas and soot yields.

Conclusions

The effects of variation in heating rate, temperature and heat flux on pyrolysis and combustion parameters of pine, cotton and wool have been investigated. Significant variations in the obtained kinetic parameter values with respect to heating rate were observed when tested between 5 and 200 K min⁻¹, and it can be suggested that this variation may be due to differences in the physical and chemical properties of each material which is even more complicated for charring materials than non-charring materials. For some charring materials such as pine, a char can develop when the material is exposed to higher temperatures. Furthermore, differences in the chemical composition of the materials can contribute to the thermal decomposition process, and similar trends have also been reported by other researchers, particularly with respect to the relationship between pyrolysis and heating rate. As wool contains significant amount of sulphur as shown in Table 2, which has inhibitory effects on the combustion process, wool can behave differently than other charring materials.

For each material studied, relationships between each material parameter and heating rate were proposed through

regression analysis. The trends and relative fit of the relationships for each parameter and for all three materials were evaluated, and it is clear that all kinetic parameters of pine materials show increasing trends with respect to increasing heating rates. This is the reverse of the corresponding trends found for wool and cotton (single effective) with respect to A and E . For n , there were a very strong decreasing power trend for wool and a very strong increasing power trend for cotton (single effective). For simplicity, the average value of n across the heating range for each material may be considered.

The variation in HoR with heating rates was also observed and explained by the likelihood that a sample has less residence time for undergoing a volatilisation process at any particular temperature at higher heating rates. The values generally increase with an increasing heating rate for all three materials tested which is also consistent with comparative literature findings.

The presence of moisture contents and likely variations in char development with respect to incident heat flux may influence the combustion parameters. Additionally, moisture evaporation and char development may not be uniform through the depth of the sample during the fire test. Considering the relative trends and strength of the relationships for all combustion parameters measured, it was found that the EHoC, soot yield, CO₂ yield and char residue of pine increased with heat flux. The CO₂ yield for cotton decreased with an increase in heat flux while for wool the EHoC, soot yield, CO₂ yield decreased with an increase in heat flux.

The characterised pyrolysis and combustion parameters of a representative set of charring materials can be used as input for CFD-based fire models. These inputs can be optimised in the proposed RAMP functions where appropriate material property values represent actual conditions. Thus, it will lead to a better and more reliable simulation of real fire scenarios that invariably involve coupled pyrolysis and combustion phenomena. Future research works should apply the parameters and RAMP functions into CFD-based fire models to simulate first bench-scale fire scenarios (such as cone calorimeter tests) and then to laboratory-scale scenarios (such as ISO room which is a 2.4 m wide × 3.6 m deep × 2.4 m high room) to validate against benchmark experiments.

Acknowledgements The authors wish to acknowledge the technical and financial assistance provided by Omnii Pty Ltd, Xtralis and Scientific Fire Services. The authors also acknowledge stimulating discussions with Dr Yun Jiang of Xtralis.

Funding Ariza S. Abu-Bakar was a Ph.D. candidate of Victoria University funded by Universiti Sains Malaysia and currently employed by the same university.

References

1. Abu Bakar AS, Cran M, Moinuddin KAM. Experimental investigation of effects of variation in heating rate, temperature and heat flux on fire properties of a non-charring polymer. *J Therm Anal Calorim*. 2019;137(2):447–59.
2. McGrattan K, Forney G. Fire dynamics simulator (version 4) user's guide. 4th ed. Washington: US Government Printing Office; 2006.
3. Jiang Y. Decomposition, ignition and flame spread on furnishing materials. CESARE: Victoria University; 2006.
4. National Institute of S, Technology. Fire Dynamics Simulator (FDS) and Smokeview (SMV). National Institute of Standard and Technology; 2015.
5. Nguyen QT, Ngo TD, Bai Y, Tran P. Experimental and numerical investigations on the thermal response of multilayer glass fibre/unsaturated polyester/organoclay composite. *Fire Mater*. 2016;40(8):1047–69.
6. Nguyen QT, Tran P, Ngo TD, Tran PA, Mendis P. Experimental and computational investigations on fire resistance of GFRP composite for building façade. *Compos B Eng*. 2014;62:218–29.
7. Nguyen Q, Ngo T, Tran P, Mendis P, Zobec M, Aye L. Fire performance of prefabricated modular units using organoclay/glass fibre reinforced polymer composite. *Constr Build Mater*. 2016;129:204–15.
8. Xu Q, Jin C, Majlingova A, Restas A. Discuss the heat release capacity of polymer derived from microscale combustion calorimeter. *J Therm Anal Calorim*. 2018;133(1):649–57.
9. Ragland K, Aerts D, Baker A. Properties of wood for combustion analysis. *Biores Technol*. 1991;37(2):161–8.
10. Moriana R, Vilaplana F, Karlsson S, Ribes A. Correlation of chemical, structural and thermal properties of natural fibres for their sustainable exploitation. *Carbohydr Polym*. 2014;112:422–31.
11. Bauer K, Garbe D, Surburg H. Flavors and fragrance in Ullmann's encyclopedia of industrial chemistry. Germany: VCH Weinheim; 1988. p. 144.
12. International Organization for S, inventor ISO 5660 -1 : 2002 Reaction-to-fire tests—Heat release, smoke production and mass loss rate—Part 1: Heat release rate (cone calorimeter method). Switzerland 2002.
13. Tata J, Alongi J, Carosio F, Frache A. Optimization of the procedure to burn textile fabrics by cone calorimeter: part I. Combustion behavior of polyester. *Fire Mater*. 2011;35(6):397–409.
14. Abu-Bakar AS, Moinuddin KAM, editors. Effects of variation in heating rate, sample mass and nitrogen flow on chemical kinetics for pyrolysis 2012 December 3–7. In: 18th Australasian fluid mechanics conference: Launceston, TAS.
15. Wang B, Gao B, Zimmerman AR, Zheng Y, Lyu H. Novel bio-char-impregnated calcium alginate beads with improved water holding and nutrient retention properties. *J Environ Manag*. 2018;209:105–11.
16. Zhu B, Haghi M, Nguyen A, Goud M, Yeung S, Young PM, et al. Delivery of theophylline as dry powder for inhalation. *Asian J Pharm Sci*. 2015;10(6):520–7.
17. American Society for Testing and Materials. ASTM 1354-04a, Standard Test Method for Heat and Visible Smoke Release Rates for Materials and Products Using an Oxygen Consumption Calorimeter: ASTM International, West Conshohocken, PA, www.astm.org; 2004.
18. Vyazovkin S. Isoconversional kinetics of thermally stimulated processes. Switzerland: Springer; 2015.
19. Wampler TP. Applied pyrolysis handbook. Boca Raton: CRC Press; 2006.
20. Viswanath SG, Gupta MC. Estimation of nonisothermal kinetic parameters from a TG curve by the methods of overdetermined

- system and inflection point. *Thermochim Acta*. 1996;285(2): 259–67.
21. Lautenberger C, Rein G, Fernandez-Pello C. The application of a genetic algorithm to estimate material properties for fire modeling from bench-scale fire test data. *Fire Safety J*. 2006;41(3): 204–14.
 22. Opfermann J. Kinetic analysis using multivariate non-linear regression. I. Basic concepts. *J Therm Anal Calorim*. 2000;60(2):641–58.
 23. Abu-Bakar AS. Characterization of fire properties for coupled pyrolysis and combustion simulation and their optimised use. College of Engineering and Science: Victoria University; 2015. .
 24. Matala A. estimation of solid phase reaction parameters for fire simulation. Faculty of Information and Natural Sciences: Helsinki University of Technology; 2008.
 25. Grønli MG, Várhegyi G, Di Blasi C. Thermogravimetric analysis and devolatilization kinetics of wood. *Ind Eng Chem Res*. 2002;41(17):4201–8.
 26. Liu N, Fan W. Modelling the thermal decompositions of wood and leaves under a nitrogen atmosphere. *Fire Mater*. 1998;22(3): 103–8.
 27. Mishra G, Kumar J, Bhaskar T. Kinetic studies on the pyrolysis of pinewood. *Bioresour Technol*. 2015;182:282–8.
 28. Słopiecka K, Bartocci P, Fantozzi F. Thermogravimetric analysis and kinetic study of poplar wood pyrolysis. *Appl Energy*. 2012;97:491–7.
 29. Wadhvani R, Sutherland D, Moinuddin KAM, Joseph P. Kinetics of pyrolysis of litter materials from pine and eucalyptus forests. *J Therm Anal Calorim*. 2017;130(3):2035–46.
 30. Yao F, Wu Q, Lei Y, Guo W, Xu Y. Thermal decomposition kinetics of natural fibers: activation energy with dynamic thermogravimetric analysis. *Polym Degrad Stab*. 2008;93(1):90–8.
 31. Missoum A, Gupta AK, Chen J. Global kinetics of the thermal decomposition of waste materials. July 27-August 1; Thirty-Second Intersociety Energy Conversion Engineering Conference (IECEC-97): Honolulu, HI, USA; 1997. p. 636–41.
 32. Anca-Couce A, Zobel N, Berger A, Behrendt F. Smouldering of pine wood: kinetics and reaction heats. *Combust Flame*. 2012;159(4):1708–19.
 33. Haseli Y, van Oijen JA, de Goey LPH. Modeling biomass particle pyrolysis with temperature-dependent heat of reactions. *J Anal Appl Pyrolysis*. 2011;90(2):140–54.
 34. Mui ELK, Cheung WH, Lee VKC, McKay G. Kinetic study on bamboo pyrolysis. *Ind Eng Chem Res*. 2008;47(15):5710–22.
 35. Quan C, Li A, Gao N. Thermogravimetric analysis and kinetic study on large particles of printed circuit board wastes. *Waste Manag*. 2009;29(8):2353–60.
 36. Milosavljevic I, Oja V, Suuberg EM. Thermal effects in cellulose pyrolysis: relationship to char formation processes. *Ind Eng Chem Res*. 1996;35(3):653–62.
 37. Farooq AA, Price D, Milnes GJ, Horrocks AR. Thermogravimetric analysis study of the mechanism of pyrolysis of untreated and flame retardant treated cotton fabrics under a continuous flow of nitrogen. *Polym Degrad Stab*. 1994;44(3):323–33.
 38. Wakelyn PJ, Bertoniere NR, French AD, Thibodeaux DP, Triplett BA, Rousselle M-A, et al. Chapter 9 cotton fibers. In: Lewin M, editor. *Handbook of fiber chemistry*. 3rd ed. Boca Raton: CRC Press; 2006. p. 612.
 39. Cao XX, Shen BX, Lu F, Yao Y, editors. Catalytic pyrolysis of cotton straw by zeolites and metal oxides. In: *Proceedings of the 20th international conference on fluidized bed combustion*; 2010: Springer.
 40. Chizhik AI, Shabes SV, Tsyui LL, Tetereva NG. The use of spline approximation for the interpretation of results of thermal analysis. *Polym Sci USSR*. 1979;21(7):1846–50.
 41. Tian CM, Zhang HY, Xu JZ, Pang XY, Guo HZ, Shi JR, et al. Studies on the flame retardation and thermal degradation of wool. *J Text Inst*. 1998;89(3):591–4.
 42. Popescu C, Augustin P. Effect of chlorination treatment on the thermogravimetric behaviour of wool fibres. *J Therm Anal Calorim*. 1999;57(2):509–15.
 43. Horrocks AR, Davies PJ. Char formation in flame-retarded wool fibres. Part 1. Effect of intumescence on thermogravimetric behaviour. *Fire Mater*. 2000;24(3):151–7.
 44. Park D. Evaluation of the combustion characteristics of railroad waste using a cone calorimeter. *Int J Environ Monit Anal*. 2014;2(1):27–35.
 45. Pottel H. The accumulation of flammable gases in cone calorimeter tests is responsible for flash ignition of wool and cotton samples. *Fire Mater*. 1996;20(2):107–9.
 46. Donskoi E, McElwain DLS. Approximate modelling of coal pyrolysis. *Fuel*. 1999;78(7):825–35.
 47. Li K-Y, Huang X, Fleischmann C, Rein G, Ji J. Pyrolysis of medium-density fiberboard: optimized search for kinetics scheme and parameters via a genetic algorithm driven by Kissinger's method. *Energy Fuels*. 2014;28(9):6130–9.
 48. Kissinger HE. Variation of peak temperature with heating rate in differential thermal analysis. *J Res Natl Bur Stand*. 1956;57(4): 217–21.
 49. Shi L, Chew MYL. A review of fire processes modeling of combustible materials under external heat flux. *Fuel*. 2013;106:30–50.

Publisher's Note Springer Nature remains neutral with regard to jurisdictional claims in published maps and institutional affiliations.